Bulletin 15 of the International Leonid Watch: First Global Analysis of the 1999 Leonid Storm

Rainer Arlt, Luis Bellot Rubio, Peter Brown, and Marc Gyssens

An overall activity profile of the 1999 Leonid meteor shower is presented based on the observations of 434 observers who reported 277 172 Leonids in 10 806 observing periods. A storm of Leonid activity was observed from western Asian, European, and African locations at a solar longitude of $\lambda_\odot = 235^\circ.285 \pm 0^\circ.001$, corresponding to November 18, 1999, $2^h02^m \pm 2^m$ UT with a peak equivalent ZHR of 3700 ± 100 based on 2.8-minute intervals. Solar longitudes refer to equinox J2000.0. The flux density of particles causing meteors brighter than magnitude +6.5 is 1.4 ± 0.3 particles per square kilometer and per hour. This corresponds to a number density of 5400 ± 1200 particles per 10^9 cubic kilometer. Additional maxima are found in the ZHR peak profile; one of them at $\lambda_\odot = 235^\circ.272$ or 1^h43^m UT can be associated with the cometary ejecta from the 1932 perihelion passage. The time of this peak as well as the main peak, which is caused by particles from the 1899 passage, are reproduced by particle simulations. A clear second activity outburst occurred at $\lambda_\odot = 235^\circ.87 \pm 0^\circ.04$ (November 18, 1999, $16^h \pm 1^h$ UT) with a maximum ZHR of 180 ± 20. The Leonid storm component is found to exhibit an unusual magnitude distribution with a lack of both very bright *and* very faint meteors.

1. Predictions and observational data

Although innumerable verbal reports would be worth reproducing, we have to restrict ourselves to the mere numbers in this overview of 1999 Leonid activity. A considerable number of meteor reports with 1-minute counts is available for the peak period; the same holds for many breakdowns of magnitude distributions. All observers who reported longer intervals during this period are highly encouraged to revisit their observations for possible shorter intervals according to their notes and tapes. Until December 8, 1999, we obtained the reports from 434 observers who logged 277 172 Leonids in a total of 10 806 observing intervals.

Predictions were attempted by three independent investigations of the stream evolution: Kondrat'eva and Reznikov [1] and Asher and McNaught [2,3] give the same peak time, November 18, 2^h08^m UT ($\lambda_\odot = 235^\circ.29$), whereas Brown [4] gives November 18, 2^h20^m UT ($\lambda_\odot = 235^\circ.30$).

In all these models, the major contribution to the peak comes from particles ejected from the parent comet in 1899. The results in [1–3] are based on the evolution of the dust trails Comet 55P/Tempel-Tuttle ejects at each perihelion passage and evaluates the encounter conditions when the Earth passes the meteoroid stream (do not confuse with the comet's tail which consists of much smaller particles). The closest encounter times given in [3] for the trails ejected in 1932 and 1965 are 1^h44^m and 1^h53^m UT corresponding to $\lambda_\odot = 235^\circ.273$ and $\lambda_\odot = 235^\circ.279$, respectively, but no significant activity was attributed to either of them. The work in [4] reports on full-stream models covering the evolution of the Leonid stream over a 2000-year history, simulating the actual number density of particles in the stream by a large number of model particles which is of the order of one million.

Locations in western Asia, Europe, and northern Africa were most favorable for witnessing a meteor storm of at least 500 meteors per hour, and many people at these locations were fully awarded with much higher rates at the exact time, weather permitting.

In addition, Emel'yanenko [5] expected that material ejected earlier than 1899 would produce enhanced rates near November 18, 17^h UT, corresponding to a solar longitude of $\lambda_\odot = 235^\circ.91$q. Brown [4] also suggested that some activity might be detectable near $\lambda_\odot = 236^\circ.0$, principally from high ejection velocity material (or, equivalently, from particles with small values of β, the ratio of the Sun's radiation pressure force to its gravity) from the 1866 ejection. Predictions in [3] were more specific and noted three possible additional peaks of activity—one near 19^h55^m UT ($\lambda_\odot = 236^\circ.04$) due to 4-revolution-old (1866) ejecta, one near 21^h59^m UT ($\lambda_\odot = 236^\circ.13$) due to 5-revolution-old (1833) ejecta and one near $236^\circ.16$ from 6-revolution-old (1799) ejecta. Throughout, solar longitudes refer to equinox J2000.0.

We are very much obliged to all observers who took part in this challenge of collecting the largest dataset of a single return of a meteor shower for their efforts in the field and their quick submission of observational reports:

Oriol Abellán, Yuuko Abe, Jonay Abril Torres, Seishi Akagi, Doblado Alarcón, Per Aldrich, José Abargues Alemán, Nuria Álvarez Rodriguez, Rubén Amayra Pacho, Alexandre Amorim, Laura Ángel Martinez, M.M. Ángel Sánchez, Barbara von Arb, Rainer Arlt, Big-ching Au, A. Barbero Roca, Joaquín Barberá, Juan Manuel Barro Santos, Marc Baró, Rony Barry, Luc Bastiaens, Nadya Baskakova, Angel Bellido Sobradelo, Ana María Beltrán Primo, Aitor Benavent, M.C. Benzal Pintado, M. Bernáldez, Felix Bettonvil, Abhay Bharad, Mikhail Bidnichenko, Louis S. Binder, Nicolas Biver, Maria de Guia Blanco, Antonio José Blanquer Cabra, F. Blanco, Neil Bone, Sara Bordowitz, Mohamed Bouazzaqui Miguiz, Hans Buchholtz, Eisse Pieter Bus, Amparo Cabezuelo López, Francisco Campos, Luna Campos, Salvador Cambres Cañigal, Jesús Cano Anguita, José Miguel Cano Pestaña, Beatriz Carreño Martinez, Gil Carmona, Raúl Ceballos Corredera, Lizardo Cejas Cejas, Carlos M. Celestrin Campa, Jakub Cerny, Chu-lok Chan, David Chan, Luke Chidester, Yeon-jong Choi, Antonio Coelho, Paola Contreras Muñoz, Gerardo José Cordero Vaca, Silvia Cordero Álvarez, Stefano Crivello, David Cuenca, Chen-zhou Cui, Luís A. da Silva Machado, Luiz Augusto da Silva, Haakon Dahle, Luigi d'Argliano, Shivinand Darbastwar, Mark Davis, Marc de Lignie, Goedele Deconinck, Ana Lucía Delgado Díaz, Werner Depoorter, Jose G. de Souza Aguiar, Prasad Deshpande, Peter Detterline, Ajitha Devarajan, Bhushan Dholakia, Asdai Díaz Rodriguez, Fernández Diaz, Antonio Díaz Pulido, Hans-Günter Diederich, José Pascual Domínguez, Manuel Domínguez Palma, Guillermo Egea, Shlomi Eini, Albert Escoda, Bella Espinar Frias, Ángela Estévez Megias, Bert Everaert, Ricardo Fagundo Rivero, Yuwei Fan, Gregori Farras, David Barba Fernández, Juan F. Fernández Ocaña, L. Fernández, Raul Fernandez, Ricardo Fernandez, Sonia Fernández Fdez, N. Flores, Edesio Edson Fortes dos Santos, Keiiti Fukui, Nobuyuki Fukuda, Kai Gaarder, Ofer Gabzo, Marcin Gajos, Martin Galea, V. García, David García Pallás, José Alberto García Quesada, Juan Carlos García, Mariano García Vilchez, Kalpana Gawhane, Li Gen, Petros Georgopoulos, Jaroslav Gerboš, Nandkishare Gite, George W. Gliba, Orly Gnat, Shelagh Godwin, Amit Gokhale, Sagar Gokhale, Yeshodhan Gokhle, Alexandra Golova, Juanjo Gómez Masmano, Marta Gómez, Manuel Gómez, Durán González, Oswaldo Gonzalez, A. González, Juan González Gonzalez, M. González, Noelia Gorrín Marrero, Prerana Gore, Laura Granell, Lew Gramer, Vered Grindberg, Rocío Guerrero Quintero, Cobos Guillén, Alejandra Gutiérrez Martinez, Antonio Gutierrez Corrales, Rafael Haag, Pavol Habuda, Cathy Hall, Wayne T. Hally, Joost Hartman, Marek Harman, Takema Hashimoto, Saurabh Hatwar, Roberto Haver, Lars Trygve Heen, Natalie Henche Saxon, Carlos Heredero, S. Hernández, Saray Herrera Arteaga, Arno Hesse, A. Hess, Pierre S. Hilaire, Michaela Honkova, Kamil Hornoch, Dave Hostetter, José Luis Iglesias, Oomi Iiyama, Maria Isaeva, Emre Isik, Daiyu Ito, Kiyoshi Izumi, Helle Jaaniste, R. Jiménez Martinez, Carl Johannink, Bhargav Joshi, Miguel Ángel Juárez, Eva María Juvé, Kapil Kanole, Stanislav Kaniansky, Kenya Kawabata, Elena Kayankina, Peter Kayankin, Alexander Kichizhiev, Marina Kichizhieva, Mark Kidger, Atusi Kisanuki, Hitomi Kisanuki, André Knöfel, Wakaba Kobayashi, Radek Kodousek, Albert Kong, Matej Korec, Detlef Koschny, Ralf Koschack, Jakub Koukal, Gábor Kövágó, Lukas Kral, Anton Krupnov, Rhishikesh Kulkarni, Vineet Kulkarni, Maris Kuperjanov, Karimu Kuragaki, Jan Kyselý, Sylvio Lachmann, Francisco Lambíes Cusí, Marco Langbroek, Alberto Latini, Kai-nang Lau, Ana Lázaro Guerrero, Anne-Laure Lebacq, Ping-chung Lee, Adrian Lelyen, Anna S. Levina, Robert Leyland, Qing Liang, Mihir Limaye, Michael Linnolt, Angel Rafael Lopez Sanchez, Armentario López Castillo, M. López, Javier López Valenciano, Juan Manuel López Álvarez, M. Ángeles López Ruiz, Sonia López, Yeray Lopez Delgado, Vladimir Lukić, Robert Lunsford, Hartwig Lüthen, Oisin MacConamhna, Kouji Maeda, Katuhiko Mameta, José Maria Martínez, José Alfonso dos Reis Martins, Nayade Martínez Molina, JM Marínez Nuñez, Pierre Martin, Rafael Carlos Martínez, C. Martínez Conesa, Fernando Martínez Ruiz, Antonio Martinez, José Luis Marínez, L. Martín, J.M. Martinez Núñez, Tony Markham, Jan Masiar, Joana Mateo Ruiz, Ketaki Matkar, Robert McNaught, Alastair McBeath, Ángeles Méndez García, Nahum Mendez Chazarra, Irene Merayo, Markko Meriniit, Marina Michailova, Alex Mikishev, Pavel Mikulka, Arjona Miranda, Koen Miskotte, Hidekatu Mizoguchi, Sui Mo, Amruta Modani, Macarena Molina de Armas, Sirko Molau, Marcelo Montagna, Soria Montesinos, Daniel Morales, José Morales Maestro, JM Morano, Judit Moreno, Leticia Mora, Moscoso Morillo, P. Morocho, Rafael Moreno Jiménez, Rivas Morán, Sergio Moreno Martínez, Francisco Munoz, María Elen Nájar, Francisco Naranjo, Sven Näther, Iván Navarro Martínez, JA Navarro Garay, Ilia Nazvanov, Marc Neijts, Jonathon Newton, John Newton, Delfi-Isabel Nieto Isabel, Pedro Nieto Martínez, A Nieto Martínez, Prakash Nitsure, Masahiko Ooba, Mohammad Odeh, Eran Ofek, Hiroshi Ogawa, Hiroyuki Okayasu, Masayuki Oka, Dragana Okolić, José Ortega, Kazuhiro Osada, Alexei Pace, Sachin Pansare, Arvind Paranjpye, Carlos Parra, Miguel Ángel Parrado Flores, JM. Pastor Hernández, Mukesh Pathak, José Vicente Pedrón Jiménez, Cedric Peinado, Ketan Pendse, Ruth Peñate Pacheco, Trevor Pendleton, Alfredo Pereira, Nataly Pershina, Silvia Pérez

Limiñana, Suyin Perret-Gentil, Alejandro Piedrabuena Delgado, Roman Pifl, Carles Pineda Ferré, Nikolay Pit, Dulce Plasencia, Isaac Plané, Granados Porras, Roberto Porcel, Fabricio Prieto Santos, Dmitry Pryadunenko, Tushar Purohit, Rui Qi, Francisca Quetglas, Roberto Carlos Ramos, E.S. Rangarajan, Pavol Rapavy, Simona Rapava, Ashutosh Rathor, Ina Rendtel, Jürgen Rendtel, Klar Gilberto Renner, Jacobo Requena Laborda, Francisco Reyes Andrés, Ian Rigney, Mayra Del Rio, Sabrina Rodríguez, Sergio Rodríguez, Paul Roggemans, Presentación Ros, Marion Rudolph, Jelyl Rufat, Antonio José Ruiz López, Roberto Carlos Ruiz Villena, Victor Ruiz Ruiz, Francisco Sáez, William Sager, Timur Sahýn, Chaitanya Salgarkar, L. Sánchez Garcia, Javier Sanchez, Nicolás Santiago Medina, Raul Santos Salcedo, Anastasia Satanova, Rocío Saucedo Núñez, Robin Scagell, Igor Schedrov, Olga Schedrova, René Scurbecq, Miguel Serra Martin, Shashank Shalgar, K. Shivasankar, Brian Shulist, Yi Shum, Anastasia Sierra Aguilar, Hiroyuki Sioi, Andrzej Skoczewski, Aaron Sluder, Kiko Soares, Milos Sochan, Mateo Soldado Sánchez, Manuel Solano Ruiz, Paqui Soriano García, George Spalding, Ulrich Sperberg, Jan Stancel, Michal Stancel, Umberto Mule Stagno, Kazuhiro Sumie, David Swann, Lai-chun Tai, Richard Taibi, Syoiti Tanaka, Honglin Tao, Khaled Tell, Manuel Tello Abolafia, Kazumi Terakubo, Neelima Thatte, Yasuhiro Tonomura, Rafael De Torres Carpio, Manuela Trenn, Josep M. Trigo Rodriguez, Satosi Uehara, Elena Valero Rodriguez, Javier Valero Rufino, José Alberto Valenciano Jiménez, Juan Valiente Soriano, Manuel Ángel Valadez López, Erwin van Ballegoy, Hendrik Vandenbruaene, Koen van Gorp, Markku Vanamo, Raúl Vázquez, I. Vega, Jose Miguel Velasco Fuentes, Cis Verbeeck, Jan Verbert, Rita Verhoef, Craig Anthony Vincent, Mark Vints, Catarina Vitorino, Helio Vital, Alenxander Voetskiy, Jan Wagner, Di Wang, Milos Weber, Thomas Weiland, Francisca Werner Marín, Margareta Westlund, Barbara Wilson, Jean-Marc Wislez, Guang-jie Wu, Dan Xia, Zhou Xingming, Masayuki Yamamoto, Kim S. Youmans, Maria Cruz Zafra, Petr Zajicek, Joseph Zammit, Eva Zapletalova, Michal Zapletal, George Zay, Ju Zhao, Jin Zhu, and Xiaojin Zhu,

who are from the following countries and regions:

Australia, Austria, Belgium, Brazil, Bulgaria, Canada, China, Cuba, Czech Republic, Denmark, Estonia, Finland, France, Germany, Greece, Hong Kong, Hungary, India, Ireland, Israel, Italy, Japan, Jordan, Korea, Malta, the Netherlands, Norway, Poland, Portugal, Slovakia, Spain, Switzerland, Turkey, United Kingdom, Ukraine, United States, Venezuela, and Yugoslavia.

As observations are still coming in, and since the amount of data is enormous, it may well be that one or another contribution has not been included yet in the following analysis. We will work hard on completing the data set and present a more in-depth analysis based on all the observational material in the course of the next year.

2. The population index problem

Usually, before going into the details of an activity profile of a meteor shower, we need information about the population index r versus time in order to correct visual counts for the sky conditions. The 1999 Leonids challenge us with unusual magnitude distributions. Two methods of population index determination, the regression line method and the conversion of an average magnitude distance from the limiting magnitude, yields completely different results. The first one obtains the population index from the slope of a best-fit regression line through the logarithmic true meteor numbers, i.e., the observed numbers extrapolated by perception probabilities [6]. The second method makes use of the uniqueness of the dependence of r on the mean magnitude *distance* from the limiting magnitude [7]. (Note that the mean magnitude alone does not deliver a unique r, because it is strongly affected by the sky conditions.)

The first method—applying a certain range of magnitudes of the distributions—gives a more or less constant population index of roughly $r \approx 2.3$ for the peak period between $\lambda_\odot = 235\overset{\circ}{.}2$ and $\lambda_\odot = 235\overset{\circ}{.}4$, whereas the second method—applying all meteors of the magnitude distribution—gives a sharp r-peak up to $r \approx 2.7$ near $\lambda_\odot = 235\overset{\circ}{.}29$ and values of 2.0 to 2.3 for the adjacent times. Both methods rely on an exponential distribution of the true number of meteors versus the magnitude. The discrepancy thus indicates a non-exponential distribution of true meteor numbers. A similar behavior was witnessed on November 16, 1998. We give a near-peak profile of the population index in Figure 1 obtained by the regression-line method over the magnitude range -1 to $+3$.

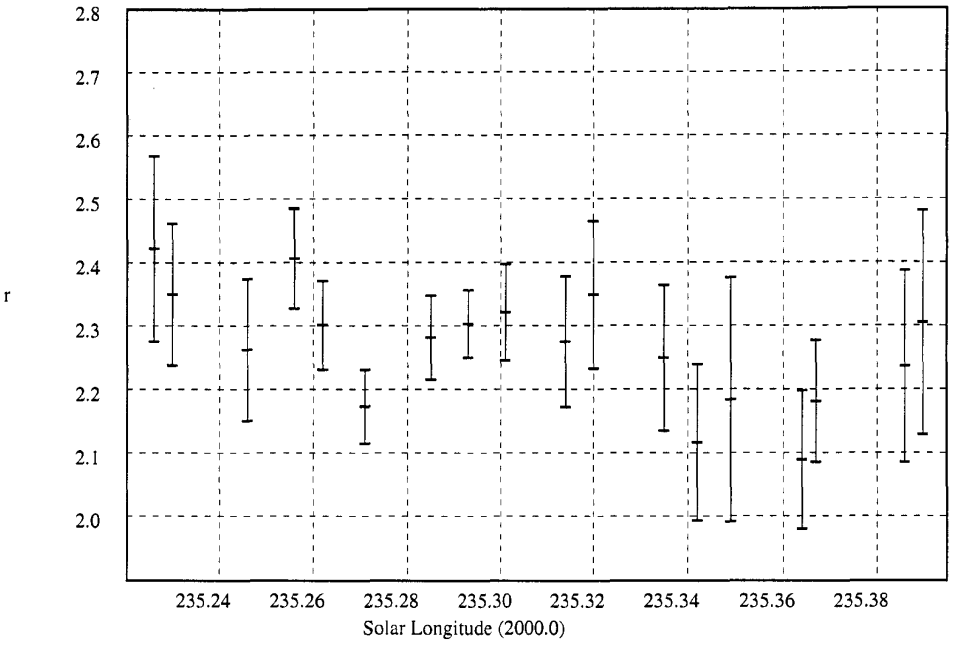

Figure 1 – Population index profile of the 1999 Leonid meteor shower peak as derived by the regression line method in the magnitude range −1 to +3. The individual r-values were averaged in bins of width 0°.02 in solar longitude, shifted by 0°.01; the mean is plotted at the average solar longitude in each bin. The error bars represent the standard deviation of the values contributing to the average.

Due to their very high geocentric velocity of 71 km/s, Leonid meteoroids as small as about 10^{-5} g are able to produce visual meteors. The distribution of true meteor numbers indeed starts to lack meteors of magnitude +4 and fainter, although the observers had the impression of an abundance of faint meteors. This impression may be subjective, however: on the one hand, due to the large total number of meteors, the number of faint ones was large, too; on the other hand, the observers noticed an obvious *lack of bright meteors*, a phenomenon many may have described *erroneously* as an *abundance of faint meteors*. Figure 2 shows the magnitude distribution of the true meteor numbers showing *both* phenomena, the lack of very faint *and* the lack of very bright meteors. The under-representation of meteors for magnitude +4 and fainter is similar to that found from video records as reported in [8]. The solid line is the total of true magnitude distributions for $\lambda_\odot = 235°.20$–$235°.30$; the dotted line refers to $\lambda_\odot = 235°.30$–$235°.40$. The deficiencies are more prominent before and during the peak than afterwards.

In view of these problems, we will adopt a population index of $r = 2.3$ for the computation of the ZHR profile and restrict the analysis to observations with limiting magnitudes between +6.0 and +7.0 to avoid large extrapolations. Even if the population index is uncertain by ±0.5, the errors introduced by the limiting magnitudes most different from +6.5 are roughly 10%. In any case, we note that the average of the individual ZHR values will be a close measure of the true activity, the large number of observations ensuring that over- and underestimated ZHRs compensate each other.

3. High-resolution activity

The great number of reports submitted to the *Visual Meteor Database* (*VMDB*) and their detailedness allow a the computation of a ZHR graph with a very fine resolution down to the order of minutes.

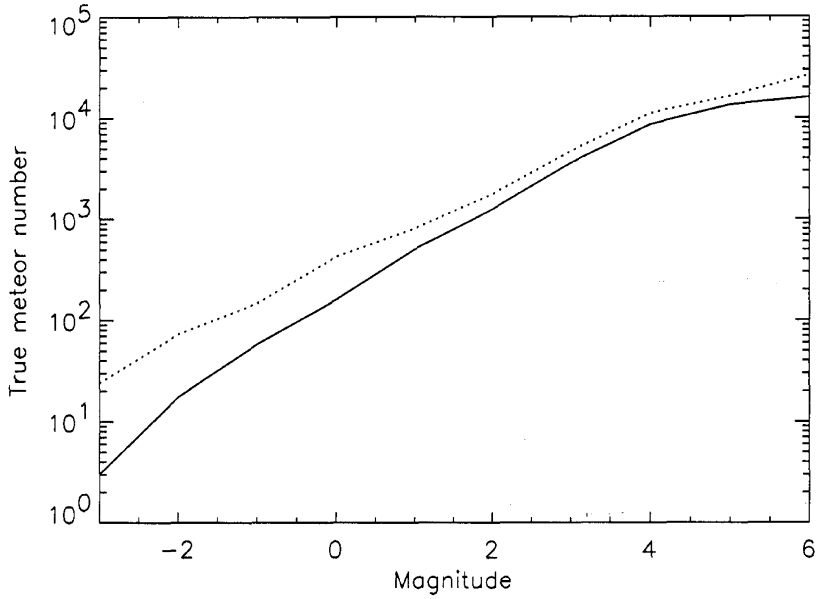

Figure 2 – Distribution of true meteor numbers corrected for perception probabilities versus magnitude for 20 experienced observers in logarithmic scale. A straight line would indicate an exponential distribution, whence the existence of a population index. The solid line refers to the period $\lambda_\odot = 235°2$–$235°3$; the dotted line to the period $\lambda_\odot = 235°3$–$235°4$.

The actual storm component in the Leonid stream is supposed to form a sheet-like structure extending approximately in the Comet's orbital plane. Since we are dealing with a temporal resolution smaller than the crossing time of the globe through this stream filament, we have to account for the actual geographic position of the observer, in order to preserve the features of the stream in the activity graph. The time shifts are called *topocentric correction*, and are described in [10]. They express the correction toward the stream encounter by the center of the Earth.

To compute this topocentric correction, each geographic position plus time is transformed into ecliptical coordinates, and the spatial offset to the direction of the center of the Earth is computed. This offset converts to a time shift given the crossing speed of the Earth through the stream.

As we encounter the stream at its descending node, the particles, which meet the Earth almost head-on, move from north to south through the ecliptic plane. Roughly speaking, southern latitudes therefore see the storm first, northern latitudes see the storm delayed. South Africa encounters the densest part 11 minutes earlier than the center of the Earth, whereas northern Scandinavia sees the peak 17.5 minutes later—6.5 minutes after topocentric encounter.

The profile near the maximum is shown in Figure 3 with a point-to-point distance of $0°.001$ in solar longitude, corresponding to 1.4 minutes. The actual binning, however, is twice as large, whence 2.8 minutes. Only observing intervals shorter than 2.8 minutes are included in each average. All activity error bars are $\mathrm{ZHR}/\sqrt{n_{\mathrm{tot}}}$, where n_{tot} is the number of Leonids involved in the average. We did not apply perception coefficients which account for personal systematic deviations of observers, since the enormous number of people ensures a reliable average. The number of individual observing intervals in each average of Figure 3 varies between 40 and 60 during the peak hours.

From Figure 3, we read the peak time as $\lambda_\odot = 235°.285 \pm 0°.001$, corresponding to November 18, 1999, $2^{\mathrm{h}}02^{\mathrm{m}} \pm 2^{\mathrm{m}}$ UT. The maximum equivalent ZHR was 3700 ± 100.

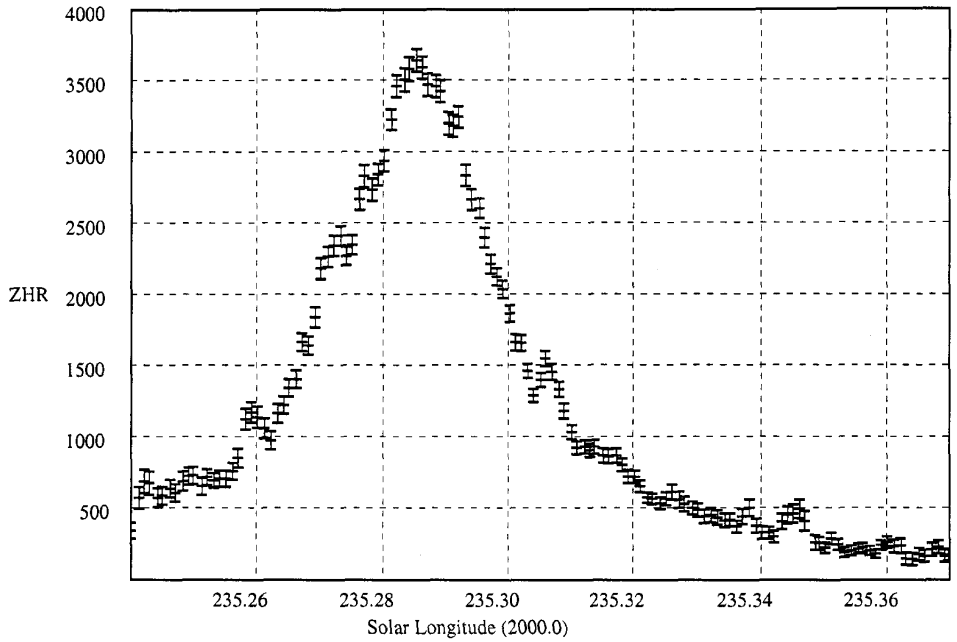

Figure 3 – ZHR-profile of the 1999 Leonid meteor storm. The time shift towards topocentric stream encounter was applied for each observing period according to [10]. Only observations with limiting magnitudes between +6.0 and +7.0 were chosen, since the derivation of a population index turned out to be almost impossible. Error bars represent $\mathrm{ZHR}/\sqrt{n_{\mathrm{tot}}}$, with n_{tot} the total number of Leonids.

Apart from the main maximum of the meteor storm shown in Figure 3, we can detect several small-scale features in the graph. Additional clear enhancements are found at $\lambda_\odot = 235\overset{\circ}{.}259$ ($1^{\mathrm{h}}25^{\mathrm{m}}$ UT), $\lambda_\odot = 235\overset{\circ}{.}272$ ($1^{\mathrm{h}}43^{\mathrm{m}}$ UT), $\lambda_\odot = 235\overset{\circ}{.}277$ ($1^{\mathrm{h}}50^{\mathrm{m}}$ UT), $\lambda_\odot = 235\overset{\circ}{.}307$ ($2^{\mathrm{h}}33^{\mathrm{m}}$ UT), $\lambda_\odot = 235\overset{\circ}{.}338$ ($3^{\mathrm{h}}17^{\mathrm{m}}$ UT), and $\lambda_\odot = 235\overset{\circ}{.}346$ ($3^{\mathrm{h}}29^{\mathrm{m}}$ UT). When grouping only locally close observing sites into "regional" profiles, these features are present in most of them. Consideration of the error bars suggests that such peaks are statistically significant with enhancements of equivalent rates of 100–300 meteors per hour above the general storm component and durations of 5 to 7 minutes. The maxima at $\lambda_\odot = 235\overset{\circ}{.}272$ and $235\overset{\circ}{.}277$ are most likely associated with the 2- and 3-revolutions-old trails, respectively, as suggested in [3], but the origin of the other, not less significant peaks remains unknown.

The full width at half maximum of the peak profile in Figure 3 is $0\overset{\circ}{.}030$ in solar longitude, or 45 minutes. This time converts to a traveling distance of the Earth of nearly 80 000 km. The extent at half number density of the storm component perpendicularly to its orbital plane is thus about 23 000 km. This value is in excellent agreement with the sizes of the trails discovered by the IRAS satellite in the wake of short-period comets at heliocentric distances of 1 AU. The Leonid ZHR was above 100 for $0\overset{\circ}{.}23$ in solar longitude, corresponding to 5.5 hours. This period is quite precisely centered on the peak time (off by only 15 minutes).

A closer look into local ZHR profiles appear to reveal structures which were not present at each site. Three examples of profiles have been compiled, grouping locations in the Near East (776 intervals with 19 089 Leonids), southern France (1110 intervals with 18 190 Leonids), and southern Spain (622 intervals with 11 116 Leonids). These examples are shown in Figure 4 with a temporal resolution of five minutes for the French and Spanish graph, and three minutes for the Near-East graph, indicating that clear differences in the structure of the profiles exist. We did not apply the time shift for topocentric stream encounter in this graph in order to preserve the original activity information provided by the observational reports.

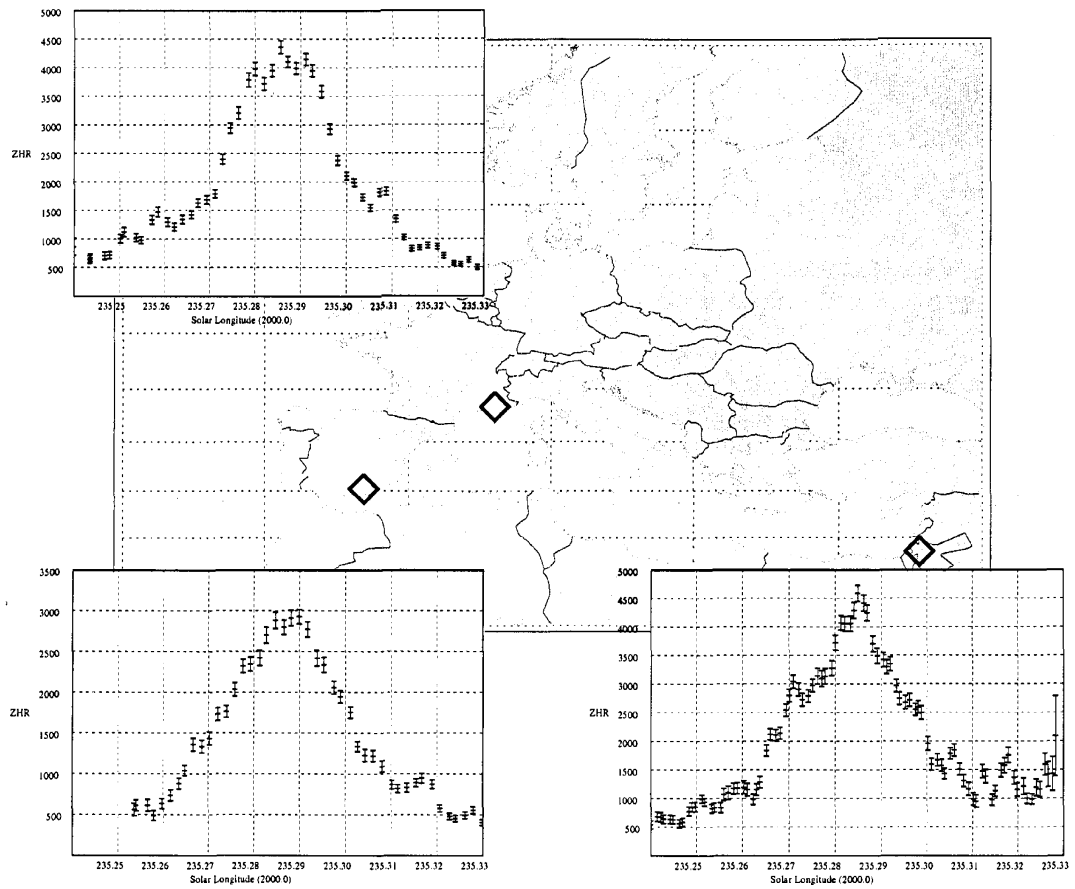

Figure 4 – ZHR profiles of peak period observer groups at different locations. The upper panel includes all observations from southern France, the lower left panel those of southern Spain, and the right panel contains all observations reported from Jordan and Israel. Again, error bars represent $\mathrm{ZHR}/\sqrt{n_{\mathrm{tot}}}$. No topocentric correction was applied to these local profiles to preserve the original results. The topocentric shifts for comparison with Figure 3 would be -1 minute ($-0^{\circ}.0007$), -2 minutes ($-0^{\circ}.0014$), and $+0.5$ minutes ($+0^{\circ}.0003$) for southern Spain, southern France, and the Near East, respectively. Only observing intervals with limiting magnitudes between 6.2 to +6.8 are included to avoid erroneous corrections due to the non-exponential magnitude distributions.

The peak time of the Spanish and the Near-East graphs differ by over 5 minutes, which is much more than the 1.5 minutes stream encounter difference expressed by topocentric correction as given in [10]. The peak time of the French graph coincides with the Near East within the resolution of the graphs, the encounter time difference being 2.5 minutes corresponding to nearly $0^{\circ}.002$ in solar longitude.

By contrast, however, a broad activity plateau of about 20 minutes duration—in a higher-resolution graph even a triple peak—is found for the observers in southern France. The strong scatter in ZHRs and the larger error bars in the Near-East graph indicate dawn interference; in contrast, the western European graphs suffer from low radiant altitudes before $\lambda_{\odot} = 235^{\circ}.26$.

The features of Figure 4 suggest that the activity also depends on the observer's geographical longitude and may provide valuable information on the structure of the dust trails parallel to the orbital plane. The wealth of data contained in these profiles means that a three-dimensional tomography of the dust trails may be attempted in the future by combining the regional activity curves.

A first attempt to derive the physical flux density of particles caught by the Earth delivers a peak value of 1.4 ± 0.3 particles causing meteors brighter than magnitude +6.5 per square kilometer and per hour. This flux density corresponds to a number density of 5400 ± 1200 particles per 10^9 cubic kilometers. The number density of particles with masses exceeding 1 mg is 230 ± 50 per 10^9 cubic kilometers at their peak. About 30 particles of 10 mg or more can be found within this volume. In contrast, 3800 particles of 10 mg or more were contained in 10^9 cubic kilometer during the Draconid outburst of early October 1998. The much higher velocity of the Leonids has two effects: (*i*) almost four times as many particles per time unit are caught by the Earth at the same number density, and, much more important, (*ii*) the high velocity causes much smaller, whence many more particles, to light up in the visual magnitude range. A Leonid particle of 10 mg produces a meteor of about magnitude 0, whereas the same particle in the Draconid stream can only produce a magnitude +6 meteor—so, we see only the biggest particles in the latter. Referring to absolute mass ranges, the spatial number density of particles found when crossing the Draconid stream is 100 times higher than at the Leonid encounter, although the peak ZHR was five times lower.

4. Late activity maximum

A significant activity peak was indeed observed close to the time predicted in [5]. East-Asian observers witnessed an outburst at $\lambda_\odot = 235\overset{\circ}{.}87 \pm 0\overset{\circ}{.}04$ (November 18, $16^h \pm 1^h$ UT) with peak ZHRs at about 180 ± 20. The actual peak value in Figure 5 comprises only six individual observing periods. A more certain value for the maximum ZHR is subject to a full analysis once all data have been utilized. When subtracting a background profile decreasing from ZHR = 55 at $\lambda_\odot = 235\overset{\circ}{.}6$ to ZHR = 30 at $\lambda_\odot = 236\overset{\circ}{.}4$, we get a full width at half maximum of $0\overset{\circ}{.}28$ in solar longitude, corresponding to 4.3 hours.

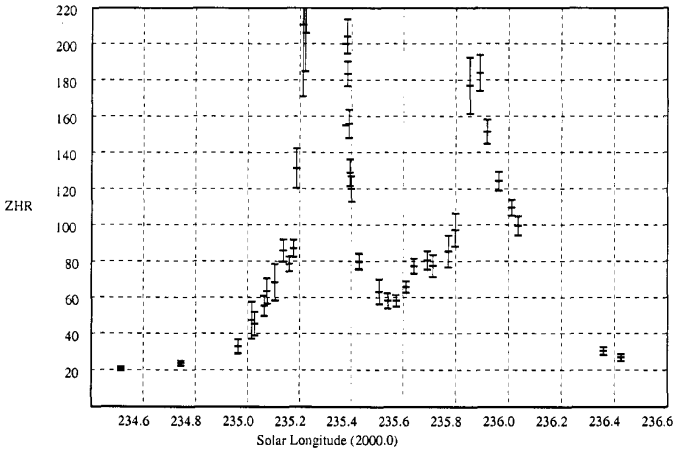

Figure 5 – ZHR-profile of the Leonids excluding their maximum.

5. Modeling of the 1999 Leonids

To attempt to reproduce the observed activity profile, the same modeling procedure used in [9] was applied to the 1999 return. The main storm profile was made up of ejecta from 1899 and 1932 only—it is possible to basically match the ZHR profile using these two ejections alone—no other epoch contributes significantly. Note that we were not able to match the observed profile using either 1899 or 1932 alone—both returns appear to have significantly contributed to the activity in 1999, within the limitations of our modeling. The ejection velocities and locations from both 1899 and 1932 epochs which resulted in Leonids close to Earth in 1999 are shown in Figure 6. All test particles within 0.002 AU of Earth's orbit (as in [9]) and one degree in mean anomaly about the nodal passage time of Earth through the stream are included.

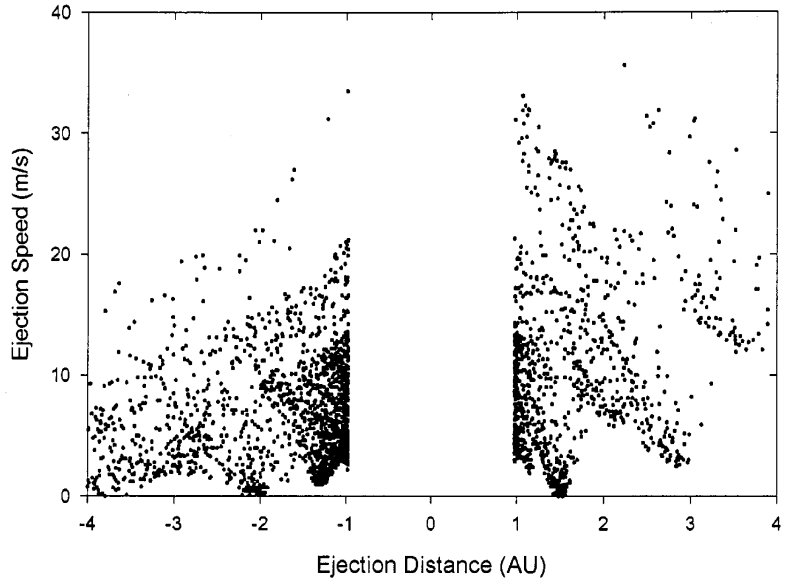

Figure 6 – Distribution of ejection velocities depending on the Comet's distance from the Sun. Negative numbers mean pre-perihelion distances. Distances closer than the perihelion distance cause the white area in the middle.

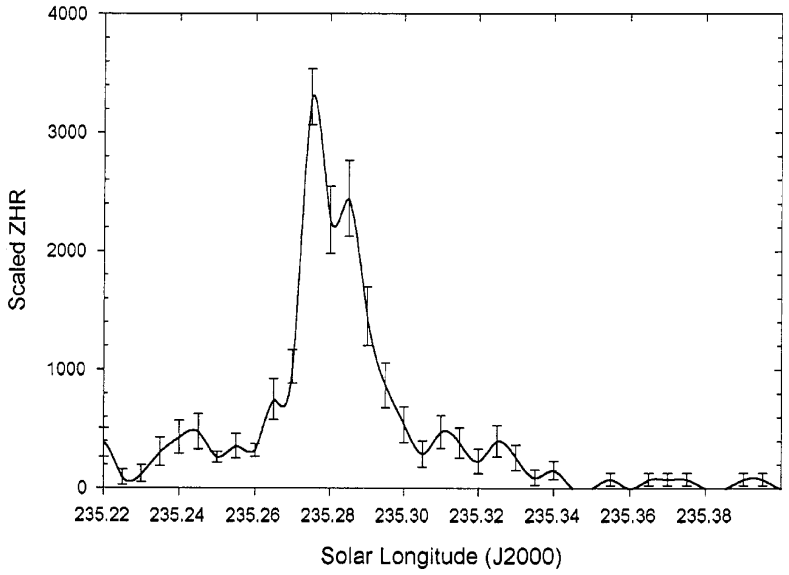

Figure 7 – Modeled ZHR profile consisting of 1899 and 1932 ejecta.

The resulting synthetic ZHR profile is found by scaling the relative activity to the observed peak ZHR in bins of 0°.005 width in solar longitude, and is shown in Figure 7. To find the relative activity from the total number of test particles accepted in each solar longitude bin, a cometary weighting exponent of 1.7 was used, as was found for Comet Halley's coma (which, for a young storm/shower, should be most appropriate—cf. [11]). The shape of the profile in this instance is relatively insensitive to the choice of the weighting exponent. We note that the model overestimates the ZHR near the early peak (due to 1932 ejecta), underestimates at the observed time of the peak, while the width of the total profile is narrower in the modeling than

is observed. As we have made a deliberate choice in the distribution of initial ejection velocities (we found that a good fit in terms of the observed profile width and timing can be obtained from a distributed coma production model using a meteoroid density of 0.8 g/cm^3—see [12] for more details), one could easily make a better fit simply by using a population with slightly larger average ejection velocities than is shown in Figure 6.

Ideally, model results which are independent of an assumed initial ejection velocity distribution could best define the delivery efficiency of material for a given ratio β and ejection velocity from 1899 and 1932. Indeed, by forcing the simulated profile to match the observed profile, it may be possible to invert results of such a simulation to obtain directly an estimate of the ejection velocities/locations which might have produced the 1999 storm, a procedure currently being examined.

Postscript: Possible lunar impacts from Leonid meteoroids

Several dedicated observers have reported possible lunar impacts caused by Leonid meteoroids (cf. the letter of Roger Venable elsewhere in this issue). Dunham [13,14] reports 6 confirmed possible impact events, mostly near the center of the Moon's dark limb. The events were registered by at least two observers and recorded on video. The 6 events occurred between 3^h05^m and 5^h16^m UT and reached magnitudes as estimated from the video frames between +3 and +7. There is still ongoing discussion on the likely sizes and masses of the meteoroids having caused these events, but it seems unlikely that they produced craters visible from Earth. Notice the discrepancy between the times of the events reported by Venable and the events reported by Dunham; there need not be a contradiction between both, however, as Venable ceased observing before the occurrence of the first event reported by Dunham. More information on the events reported by Dunham, as well as video images, can be found at `http://iota.jhuapl.edu`.

Interestingly, Asher [14] calculated that the minimal distance between the Moon and the core of the 3-revolutions-old (1899) trail was +0.0002 AU (outside the trail's orbit), compared to −0.0064 AU for the Earth (inside the trail's orbit). This makes the encounter geometry for the Moon quite comparable with that for the Earth during the 1833 and 1966 storms! Therefore, the Moon experienced a substantially higher Leonid flux than the Earth in 1999. According to Asher, the Moon's closest approach to the core of the 3-revolutions-old trail occurred 161 minutes after the Earth's closest approach. Adding this to the peak time obtained from this analysis yields November 18, 4^h43^m UT, as the time of peak encounter for the Moon.

References

[1] E.D. Kondrat'eva, E.A. Reznikov, "Comet Tempel-Tuttle and the Leonid Meteor Swarm.", *Sol. Syst. Res.rm 19*, 1985, pp. 96–101.

[2] D. Asher, "The Leonid Meteor Storms of 1833 and 1966", *Mon. Not. R. Astr. Soc.* 307, 1999, pp. 919–924.

[3] R.H. McNaught, D.J. Asher, "Leonid Dust Trails and Meteor Storms", *WGN* 27, 1999, pp. 85–102.

[4] P. Brown, "Evolution of Two Periodic Meteoroid Streams: The Perseids and Leonids", Ph. D. Thesis, Univ. of Western Ontario, London, Ont., 1999, pp. 171–258.

[5] V. Emel'yanenko, *personal communications*, November 1999.

[6] R. Koschack, J. Rendtel, "Determination of Spatial Number Density and Mass Index from Visual Meteor Observations (II)", *WGN* 18, 1990, pp. 119–140.

[7] R. Arlt, "Global Analysis of the 1998 Perseid Meteor Shower", *WGN* 27, 1999, pp. 237–249.

[8] S. Molau, J. Rendtel, M. Nitschke, "First Results of Video Observations during the 1999 Leonid Storm", *WGN* 27, 1999, pp. 296–300.

[9] R. Arlt, P. Brown, "Bulletin 14 of the International Leonid Watch: Final Results of the 1998 Leonid Meteor Shower", *WGN* 27, 1999, pp. 267–285.

[10] R.H. McNaught, D.J. Asher, "Variation of Leonid Maximum Times with Location of Observer", *Meteorit. Planet. Sci.* 34, 1999, pp. 975–978.

[11] P. Brown, J. Jones, "Simulation of the Formation and Evolution of the Perseid Meteoroid Stream", *Icarus* 133, 1998, pp. 36–68.

[12] J.A.M. McDonnell, G.C. Evans, S.T. Evans, W.M. Alexander, W.M. Burton, J.G. Firth, E. Bussoletti, R.J.L. Grard, M.S. Hanner, Z. Sekanina, "The Dust Distribution within the Inner Coma of Comet P/Halley 1982 *i*–Encounter by Giotto's Impact Detectors", *Astron. Astrophys.* 187, 1987, pp. 719–741.

[13] *IAU Circular* 7320, November 26, 1999.

[14] D. Dunham, *electronic communication* through various mailing lists, December 1999.

[15] D. Asher, *personal communications*, December 13, 1999.